Available online at www.sciencedirect.com
SCIENCE DIRECT®
Journal of Sound and Vibration 289 (2006) 245–263
JOURNAL OF SOUND AND VIBRATION
www.elsevier.com/locate/jsvi

Modeling of automotive drum brakes for squeal and parameter sensitivity analysis

Jinchun Huang, Charles M. Krousgrill, Anil K. Bajaj*

School of Mechanical Engineering, 585 Purdue Mall, Purdue University, West Lafayette, IN 47907-2088, USA

Received 20 July 2004; received in revised form 25 January 2005; accepted 5 February 2005
Available online 26 April 2005

Abstract

Many fundamental studies have been conducted to explain the occurrence of squeal in disc and drum brake systems. The elimination of brake squeal, however, still remains a challenging area of research. Here, a numerical modeling approach is developed for investigating the onset of squeal in a drum brake system. The brake system model is based on the modal information extracted from finite element models for individual brake components. The component models of drum and shoes are coupled by the shoe lining material which is modeled as springs located at the centroids of discretized drum and shoe interface elements. The developed multi degree of freedom coupled brake system model is a linear non-self-adjoint system. Its vibrational characteristics are determined by a complex eigenvalue analysis. The study shows that both the frequency separation between two system modes due to static coupling and their associated mode shapes play an important role in mode merging. Mode merging and veering are identified as two important features of modes exhibiting strong interactions, and those modes are likely candidates that lead to coupled-mode instability. Techniques are developed for a parameter sensitivity analysis with respect to lining stiffness and the stiffness of the brake actuation system. The influence of lining friction coefficient on the propensity to squeal is also discussed.
© 2005 Elsevier Ltd. All rights reserved.

*Corresponding author. Tel.: +1 765 494 6896; fax: +1 765 494 0539.
E-mail address: bajaj@ecn.purdue.edu (A.K. Bajaj).

0022-460X/$ - see front matter © 2005 Elsevier Ltd. All rights reserved.
doi:10.1016/j.jsv.2005.02.007

1. Introduction

Automotive brake noise and vibration control has become increasingly important for the improvement of vehicle quietness and passenger comfort. Over the years, brake noise has been classified by frequency contents and given various names such as grunt, judder, moan, groan, squeal, squeak and so on. In a recent review on disc brake squeal, Kinkaid et al. [1] stated that there has not been a precise definition of brake squeal. Since Nishiwaki [2] showed that groan and squeal are generated by the same phenomenon of dynamic instability, both low- and high-frequency noise can be studied by using the same modeling and analysis techniques. Brake squeal here is defined as any type of elastic instability that involves elastic modes of various brake components and is within the audible range of frequencies.

Systematic research on brake squeal can be traced back to the 1950s and still is an active subject for current researchers and engineers. The structure of brakes which consist of several components is complicated, and the fugitive nature of friction makes the problem more difficult. Research on brake squeal has been conducted using theoretical, experimental, and computational approaches. Many theoretical approaches have been presented to explore the squeal mechanisms. Early attempts to explain brake squeal emphasized that the negative slope of the friction coefficient with respect to the relative velocity caused the self-excited vibration. Spurr [3] proposed the sprag-slip model to introduce a new mechanism called geometry instability, without including the friction characteristic. Millner [4] also reported that brake squeal may occur even if the friction coefficient is constant. North [5] first presented a simple 2-dof model, in which the friction leads to an asymmetric stiffness coupling indicating non-conservative forces and the instability may occur. This mechanism was developed and advanced by many other investigators, and in this approach it is believed that brake squeal is mainly caused by dynamic instability of the brake system with variable friction forces [6,7].

In recent years the main focus on brake squeal problems has shifted from fundamental theoretical research to more practical and problem-solving oriented efforts. Instead of a simple schematic model, the brake system model tends to include more brake components, and the effects of design parameters on the stability can be investigated. Liles [8] created a linear system model based on the modal information of the disc brake components, and performed a complex eigenvalue analysis to solve the equations of motion. Guan and Jiang [9] constructed a coupled linear model including all disc brake components and identified the substructure modes which have great influence on the system stability. Chowdhary et al. [10] developed an assumed modes model for squeal prediction of a disc brake, and found that the separation between the frequencies is an important factor in determining the onset of flutter-type instability. Ouyang et al. [11] considered the effects of rotation of the disc, and the friction-induced vibration of the disc brake was treated as a moving load problem. With the improvement of numerical techniques, Hamabe et al. [12] and Nack [13] directly conducted a complex eigenvalue analysis with a finite element (FE) model of a brake system including the friction force. In their work on disc brake squeal using FE analysis, Lee et al. [14] performed a nonlinear contact analysis to determine the pressure distribution at the friction interface followed by system linearization and a complex modal analysis. Thus, in their study, the contact stiffness was dependent on local contact pressure.

In the present work, a numerical approach is presented to study the drum brake squeal. FE models are first created for brake components including the drum and the shoes. The shoe lining is

modeled as a layer having a distributed compliance that produces a stiffness coupling between the drum and shoes. There are two components of this coupling, one corresponding to transverse displacements and the other due to tangential forces arising as a result of friction coupling between drum and the shoes. The total degrees of freedom are reduced by transforming the physical coordinate model into a modal coordinate model. The resulting system model has symmetric as well as asymmetric stiffness matrices, and a complex eigenvalue analysis is carried out to determine the stability characteristics of the brake assembly. It is seen that eigenvalue veering and compatible mode shapes for the coupled drum brake system without friction are necessary conditions for brake squeal to occur in the presence of friction. To authors' knowledge, this is the first instance when eigenvalue-loci veering and strong modal coupling are clearly identified as necessary conditions for coupled-mode instability to arise. Based on this model, the influences of the friction coefficient, the lining stiffness, and the hydraulic cylinder stiffness on system stability are discussed.

2. Modeling of drum brake system

The procedure to create a linear brake system model includes the following steps: constructing FE models for brake components, performing modal analysis and extracting the modal information (frequencies and mode shapes), adding the effects of lining stiffness and friction forces, and finally incorporating the effects of boundary conditions to form a coupled model.

Four major components participate in the vibrational response of a drum brake system [15]: the drum, the brake shoes, the shoe lining, and the backing plate. The shoe linings attached on the shoes are in contact with the drum to generate radial as well as friction forces during braking. The two shoes are connected by two hydraulic cylinders. Each of the cylinders contains two floating pistons to activate the shoes in any braking action. The type of drum brake system under consideration is illustrated in Fig. 1. The shoes rest on the backing plate and are thus constrained in z direction (out of the plane of the paper).

Previous research on drum brake squeal has shown that friction-induced vibration is generated by the stiffness and friction coupling between the drum and the shoes through the shoe lining. Even though the backing plate vibrates with a large amplitude and may even be responsible for a large fraction of the noise generated by the brake system, it is believed to be not an essential contributor to the friction-induced instability in drum brakes. Thus, the simplified coupled model only includes the drum, the shoes, and the shoe lining, while the effect of the backing plate stiffness is incorporated in the boundary conditions. See Servis [15] for a comprehensive review of literature on drum brake squeal.

FE models are generated in ANSYS® for these components using three-dimensional brick elements (solid 45). Models of the drum and the shoe used for analysis are shown in Figs. 2 and 3. The drum is clamped in the bolt hole positions while the shoe model uses free boundary conditions. To include the inertial and stiffness influences of the shoe lining on modal characteristics (modal frequencies and shapes) of the shoe, the shoe lining is modeled as an integral part of the FE model of the shoe.

Each component's FE model is refined and adjusted to make the analytical results close to experimental modal analysis results [9,15]. An accurate representation of the component models as well as the statically coupled model [16] is important for good correspondence between

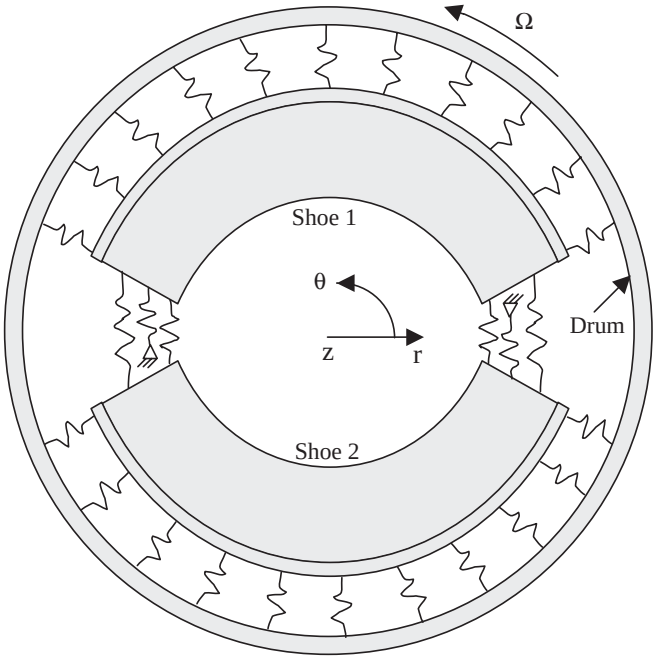

Fig. 1. Schematic of a drum brake system.

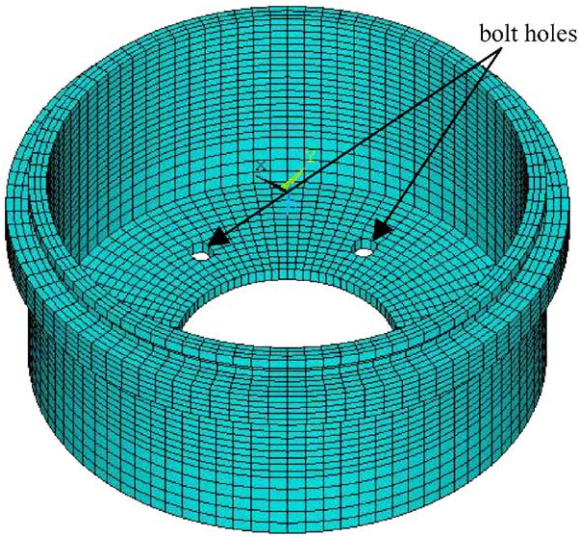

Fig. 2. FE model of the brake drum.

experimental squeal characteristics and those in simulations because the brake system's propensity to squeal is very sensitive to the geometry of the system and the material properties. Then the natural frequencies and mass-normalized mode shapes for each component are extracted from the modal analysis of the FE models. These modal characteristics of the components are used to

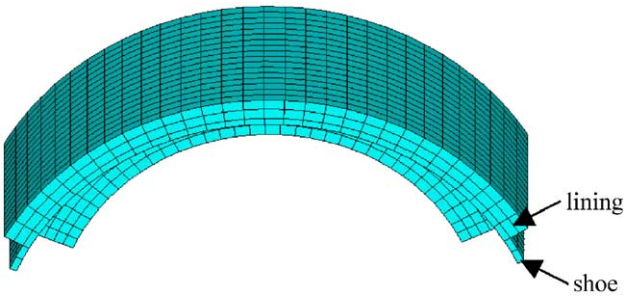

Fig. 3. FE model of a brake shoe with lining.

replace the FE models to form the coupled system, and the total degrees of freedom are greatly reduced. To ensure the accuracy of the modal representations of the components and the convergence of the stability analysis results, the upper cut-off frequency for individual component modes was selected at least as high as twice of the squeal frequency of interest. It was found that for a system model constructed in this manner, the frequencies of the statically coupled drum-shoes-lining system exhibited convergence in the range of interest. More specifically, for the results reported later in this work, 50 modes of the drum up to frequency 6271 Hz and 50 modes of each of the shoe up to frequency 8522 Hz were retained in the model.

The equations of motion of the uncoupled system including one drum and two identical shoes can be written as

$$\{\ddot{q}\} + [\omega^2]\{q\} = \{0\}, \tag{1}$$

where $[\omega^2]$ is a diagonal matrix of the extracted N natural frequencies of the components, and $\{q\}$ is an N-vector of generalized coordinates. The number of degrees of freedom of the system, N, is equal to the total number of extracted component modes.

The next step in the system modeling process is to consider the coupling between the drum and each shoe through the shoe lining. As shown in Fig. 4, the contact interface between the drum and shoe is first discretized into a mesh of M two-dimensional contact elements, which are not necessarily the same as the elements in the FE models. The lining material is then modeled as a series of discrete springs located at the centroids of contact elements. The stiffness of each spring is the total stiffness of the lining in contact with the contact element, and can be found by

$$k_n = E_{\text{lin}} * A_n / h_{\text{lin}}, \tag{2}$$

where k_n and A_n represent the spring stiffness and the area of the nth element respectively, and E_{lin} and h_{lin} are the Young's modulus in radial direction and thickness of the lining, respectively. E_{lin} is dependent on the contact pressure at the friction interface. The interface pressure distribution is in turn dependent on the actuation loads and the contact condition, and generally is non-uniform [17,18]. To make it easy to focus on the effects of friction coupling and to simplify the analysis, E_{lin} is assumed to be uniform in the first approximation. After fully understanding the mechanism of brake squeal, non-uniform Young's modulus of the lining can be incorporated into the system model without any technique difficulties. Since the stiffness of each spring element depends on the area of the contact element, the stiffness of the springs can also be non-uniform if the mesh is not uniform. Furthermore, this approach allows for the flexibility of incorporating effects of

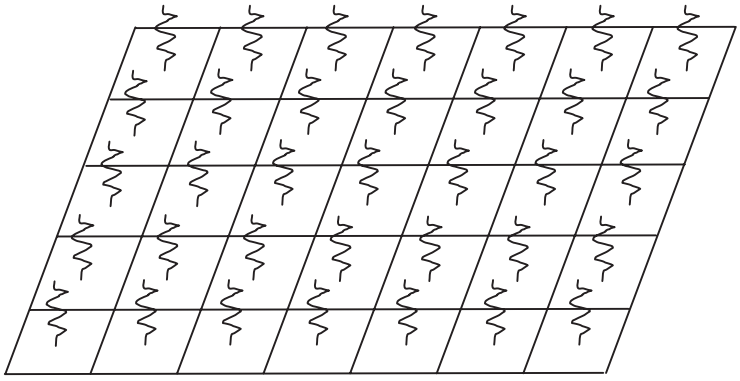

Fig. 4. Discretization of contact interface between the shoe and the drum, and its representation by equivalent springs.

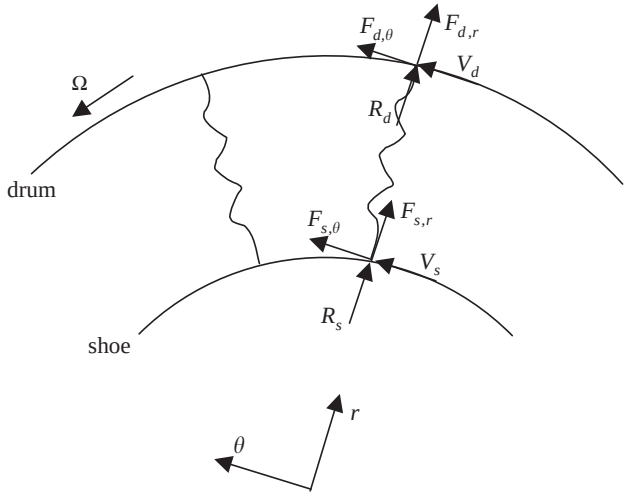

Fig. 5. Force diagram at the nth lining spring element.

modification in lining geometry often incorporated as practical measures to reduce propensity to squeal. These include chamfered lining pads as well as pads with segmentations.

The spring force and the friction force generated at each contact element can be expressed in terms of component displacements at the centroid of the element. For example, as shown in Fig. 5, the forces for the nth element at the interface between the drum and a shoe can be written as

$$\{\hat{F}_n\} = \begin{Bmatrix} F_{d,r} \\ F_{d,\theta} \\ F_{s,r} \\ F_{s,\theta} \end{Bmatrix} = \left[\begin{bmatrix} -k_n & 0 & k_n & 0 \\ 0 & 0 & 0 & 0 \\ k_n & 0 & -k_n & 0 \\ 0 & 0 & 0 & 0 \end{bmatrix} + \mu \begin{bmatrix} 0 & 0 & 0 & 0 \\ k_n & 0 & -k_n & 0 \\ 0 & 0 & 0 & 0 \\ -k_n & 0 & k_n & 0 \end{bmatrix} \right] \begin{Bmatrix} R_d \\ V_d \\ R_s \\ V_s \end{Bmatrix}$$
$$= -[[\hat{A}_n] + \mu[\hat{B}_n]]\{\hat{U}_n\}, \tag{3}$$

where R_d and V_d are the displacements of the centroid of the nth element on the surface of the drum in r and θ direction, respectively, and R_s and V_s are those of the shoe. V_d represents the contribution of the linear vibration about an equilibrium state, in which the shoes are steadily sliding over the rotating drum surface after the brake is applied. Note here that the possible component of friction force in z direction is neglected in the model as the slip velocity is essentially in the θ direction.

The same procedure is repeated for each contact element, and the combination of all these force vectors results in

$$\{\hat{F}\} = -[[\hat{A}] + \mu[\hat{B}]]\{\hat{U}\}. \tag{4}$$

Here the $[\hat{A}]$ and $[\hat{B}]$ matrices are composed of the elemental contact matrices $[\hat{A}_n]$ and $[\hat{B}_n]$, with $n = 1, 2, \ldots, M$, as submatrices.

In order to incorporate the interface forces into the system model, the coordinate transformation between the displacement coordinates $\{\hat{U}\}$ and the system generalized coordinates $\{q\}$ is

$$\{\hat{U}\} = [\hat{\Phi}]\{q\}, \tag{5}$$

where $[\hat{\Phi}]$ is a non-square matrix containing the component mode shape deformations at the centroids of the contact elements. Since each contact element force vector contains two components (normal and tangential) and the braking system has contact between each shoe and the drum, $[\hat{\Phi}]$ is a $4M \times N$ matrix. The centroid mode shape deformation can be obtained by a linear interpolation of the mode shape deformations of contact element nodes. In this way, the proposed approach does not require the FE meshes of the drum and shoes in the contact area to match, hence simplifying the FE modeling of the components.

Substituting Eq. (5) into Eq. (4) and premultiplying by $[\hat{\Phi}]^{\mathrm{T}}$ produces the generalized forces $\{f_1\}$ in the model that arise due to the normal and frictional forces at the interface:

$$\{f_1\} = [\hat{\Phi}]^{\mathrm{T}}\{\hat{F}\} = -[[A] + \mu[B]]\{q\}, \tag{6}$$

where

$$[A] = [\hat{\Phi}]^{\mathrm{T}}[\hat{A}][\hat{\Phi}]; \quad [B] = [\hat{\Phi}]^{\mathrm{T}}[\hat{B}][\hat{\Phi}]. \tag{7,8}$$

Other component interconnections are also considered. These include the constraints imposed by the hydraulic cylinders for the brake shoes at points of brake actuation, and the constraints imposed on the shoes by their rest points on the backing plate. Thus, the axial compliance of the hydraulic cylinders between the ends of each shoe is modeled as linear springs connecting the two shoes. In order to include the contact stiffness between the shoes and the backing plate, springs are used to connect the shoes to the ground in both z and θ directions. The contact between the shoes and the backing plate is assumed to be smooth, and no friction force is included at these interfaces. Proper hydraulic and backing plate stiffnesses can be obtained through validation of the coupled model to match the computational coupled frequencies with the experimental results. Using a procedure similar to the one used for the lining coupling, the force vector due to both of the above mentioned stiffness boundary conditions can be written as

$$\{f_2\} = -[C]\{q\}. \tag{9}$$

The linear equations of motion for the complete coupled brake system are formed by combining the uncoupled system (1) with the force vectors in Eqs. (6) and (9), and can be written as

$$\{\ddot{q}\} + [[\omega^2] + [A] + \mu[B] + [C]]\{q\} = \{0\}. \tag{10}$$

In summary, $[A]$ and $[C]$ are stiffness contributions due to the lining and shoe supports, respectively. Since generalized forces corresponding to these matrices are conservative, $[A]$ and $[C]$ are both symmetric and positive semi-definite. The matrix $[B]$ arises from friction coupling between the shoes and the drum. The fact that the corresponding generalized forces are non-conservative is reflected in the $[B]$ matrix being asymmetric.

The vibrational and stability characteristics of the coupled brake system can be then determined from the eigenvalue problem corresponding to Eq. (10):

$$[\lambda^2[I] + [\omega^2] + [A] + \mu[B] + [C]]\{r\} = \{0\}, \tag{11}$$

where $\{q\} = \{r\}e^{\lambda t}$.

In the absence of lining coupling (i.e., $[A] = [0]$ and $\mu = 0$), the eigenvalues are purely imaginary with the imaginary parts being the natural frequencies of the drum component and of the shoes coupled through the hydraulic cylinder stiffness and backing plate stiffness. Note that the corresponding eigenvectors can then be used to reconstitute the elastic modes of the brake system. In the presence of lining stiffness coupling but no friction coupling, the eigenvalues are again purely imaginary and correspond to the natural frequencies of an engaged brake system which is not rotating (since no friction forces act between the drum and shoes). This will be referred to as the "statically coupled" system. In the presence of both stiffness and friction coupling in the lining (i.e., the complete form of Eq. (11)), the eigenvalues are no longer guaranteed to be purely imaginary since $[B]$ is asymmetric. When all of the eigenvalues are purely imaginary, these correspond to the natural frequencies of an engaged and rotating system. If any of the eigenvalues is complex, it will appear in the form of complex conjugate pairs, one with positive real part and the other with negative real part. The existence of complex roots with positive real parts indicates the presence of a "mode-merging" (or "coupled-mode" flutter) instability, which causes brake squeal. The value of friction coefficient μ that demarcates stable and unstable oscillations will be referred to as a "critical value" of friction coefficient, μ_{cr}. The imaginary part of the eigenvalue with a double root at this μ_{cr} is the "squeal" frequency, and the corresponding reconstituted elastic mode of the complex structure is the mode shape at squeal.

3. Analysis of the coupled model

The numerical results presented in this work correspond to a drum brake system described by the parameters given in Table 1. The material properties for the drum, the shoes, and the lining used in the FE model are given in Table 2. For this system, a total of 150 component modes were incorporated into the coupled model. These include the first 50 modes each for the drum and the two shoes. These modes include six rigid body modes for each shoe, modes up to the natural frequency of 6271 Hz for the drum, and non-rigid body modes up to frequency 8522 Hz for the shoes.

Table 1
Nominal values of system geometric parameters

Parameter	Symbol	Value
Inner radius of drum ring	r_d	0.160 m
Width of drum ring	w_d	0.148 m
Height of drum ring	h_d	0.012 m
Thickness of drum cap	h_c	0.009 m
Inner radius of drum cap	b_c	0.075 m
Arc length of shoe	γ_s	132.8°
Width of shoe top	w_t	0.102 m
Height of shoe top	h_t	0.0038 m
Width of shoe rib	w_s	0.006 m
Height of shoe rib	h_s	0.032 m
Arc length of lining	γ_{lin}	120°
Width of lining	w_{lin}	0.1 m
Thickness of lining	h_{lin}	0.011 m

Table 2
Nominal values of material parameters

Parameter	Symbol	Value
Density of drum material	ρ_d	7250 kg/m^3
Young's modulus of drum	E_d	1.1×10^{11} N/m^2
Density of shoe material	ρ_s	7860 kg/m^3
Young's modulus of shoe	E_s	2.1×10^{11} N/m^2
Density of lining material	ρ_{lin}	1650 kg/m^3
Young's modulus of lining (in radial direction)	E_{lin}	2.1×10^{8} N/m^2

For the results presented in Sections 3.1 and 3.2, the hydraulic cylinder stiffness and backing plate contact stiffness are set to equal zero. The primary purpose here is to understand the influences of mode merging and veering on the occurrence of brake squeal, and this understanding is independent of brake types and boundary conditions. Their effects will be considered in a later section.

3.1. Effect of the friction coefficient

To study the influence of friction, the complex eigenvalue analysis of Eq. (11) was conducted using the nominal lining stiffness derived from Tables 1 and 2. The variations of the frequencies (or imaginary parts of the eigenvalues in case of complex frequencies) of modes 20–32 (lying in the range of 2100–2900 Hz) with the friction coefficient μ are shown in Fig. 6. These mode numbers are identified in terms of the ordering of eigenvalues for the statically coupled modal model. For this nominal system, there are no other modes that exhibit any instability in the range of $0 < \mu < 0.5$.

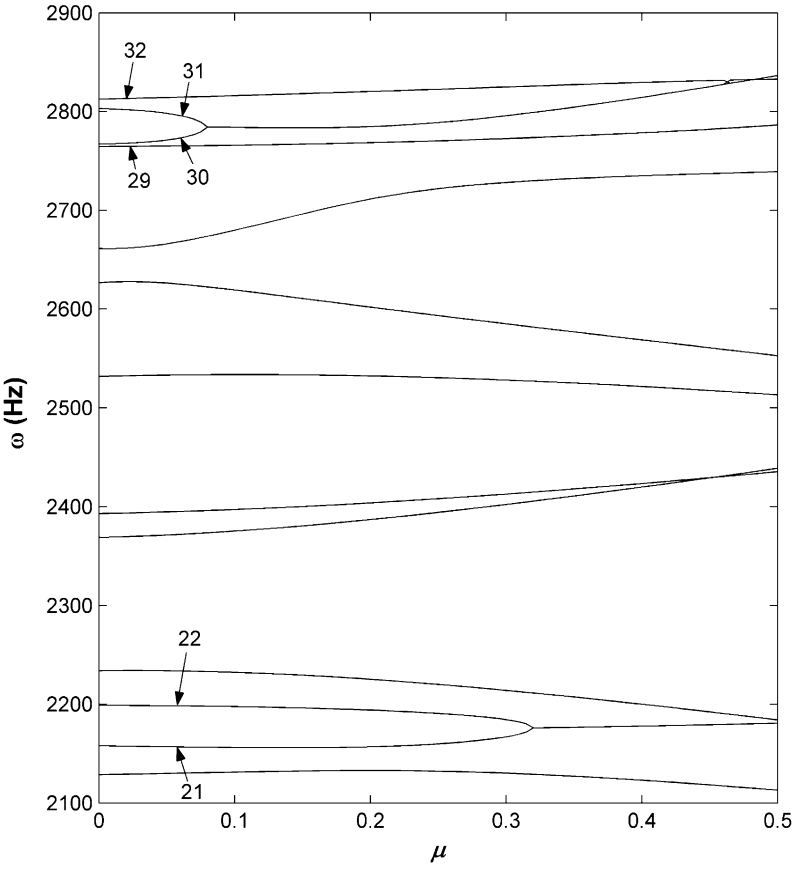

Fig. 6. Variation of the frequencies (or imaginary parts of the eigenvalues in case of complex frequencies) with μ.

Both the frequencies and mode shapes change when friction coefficient varies. At the critical value of friction coefficient, a pair of modes merge, i.e., their frequencies and mode shapes become identical. This merging state defines the onset of squeal.

Two occurrences of mode-merging instability are observed in the frequency range and range of friction coefficients presented in Fig. 6. One mode-merging occurs between modes 21 and 22 near $\mu_{cr} = 0.32$. Note that for each mode of the system, the components of the system are oscillating with a specific shape distribution. The shapes of these two modes for $\mu = 0$ are dominated by the bending modes of drum side wall and shoe components. When μ is slightly larger than μ_{cr}, the corresponding eigenvalues become complex, with imaginary parts ("squeal frequency") near 2176 Hz. A second mode merging occurs between modes 30 and 31 near $\mu_{cr} = 0.08$, with shapes of these two modes at $\mu = 0$ being dominated by the torsional modes of drum side wall and shoe components. The squeal frequency for this mode merging is near 2784 Hz. Among the various critical values of μ for different frequency pairs, the minimum one ($\mu_{cr,min}$) is the most important and defines the stability boundary for a brake system. The squeal modes for the nominal drum brake system for these two critical values of μ are presented in Fig. 7. Recall that at a critical value

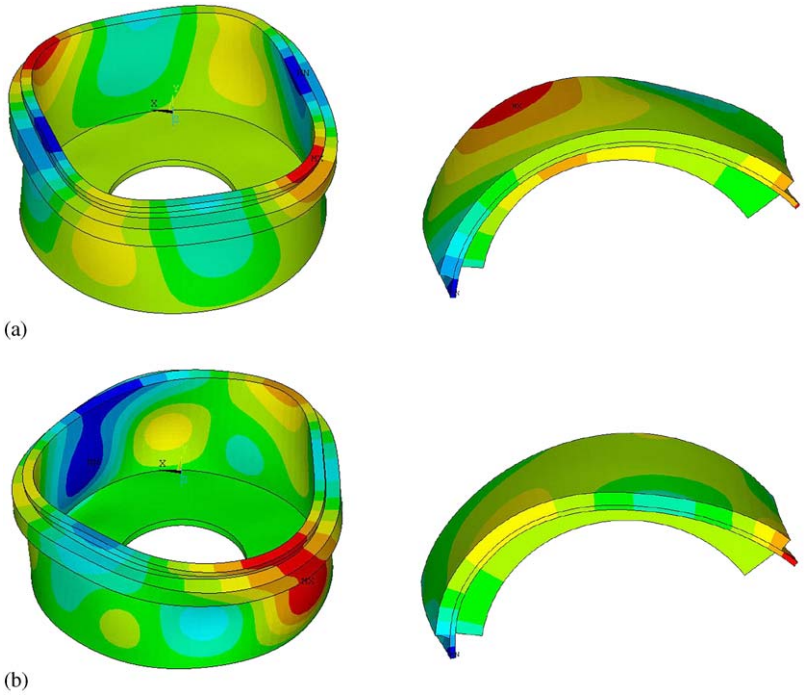

Fig. 7. Mode shapes at onset of squeal for two different critical values of μ: (a) mode shapes of the coupled drum brake system when modes 21 and 22 have merged; (b) mode shapes of the coupled drum brake system when modes 30 and 31 have merged.

of μ, two distinct modes have merged and have the same natural frequencies and identical mode shapes.

To explain why brake squeal occurs at some specific and distinct frequencies, many investigators have conducted experimental investigations [6,19]. In these experiments it is found that squeal frequencies are often close to natural frequencies of one or more of the components or near some natural frequencies of the statically coupled system. Since both the frequencies and mode shapes change as the brake is engaged, and further change as the friction is included, it may be difficult to identify which component modes lead to squeal. Moreover, there are many more component modes in a brake system, and it is difficult to explain why squeal occurs only at a few frequencies.

Chowdhary et al. [10] in their work with disc brakes found that the modes with the least separation due to static coupling tend to merge and become complex for higher values of μ. This conclusion agrees with the fact that usually the neighboring modes with close frequencies or the pairwise modes arising due to components symmetry tend to merge.

It can be seen from Fig. 6 that modes 29 and 30 have the smallest separation at $\mu = 0$; however, mode 30 is seen to merge with mode 31 rather than with mode 29. It is expected that the shapes of a pair of modes also play an important role in mode merging in addition to the closeness of their frequencies. Consider the radial components of the statically coupled system's mode shapes for modes 29–32, or more specifically the modal deformations of the drum and a shoe in these modes (see Fig. 8).

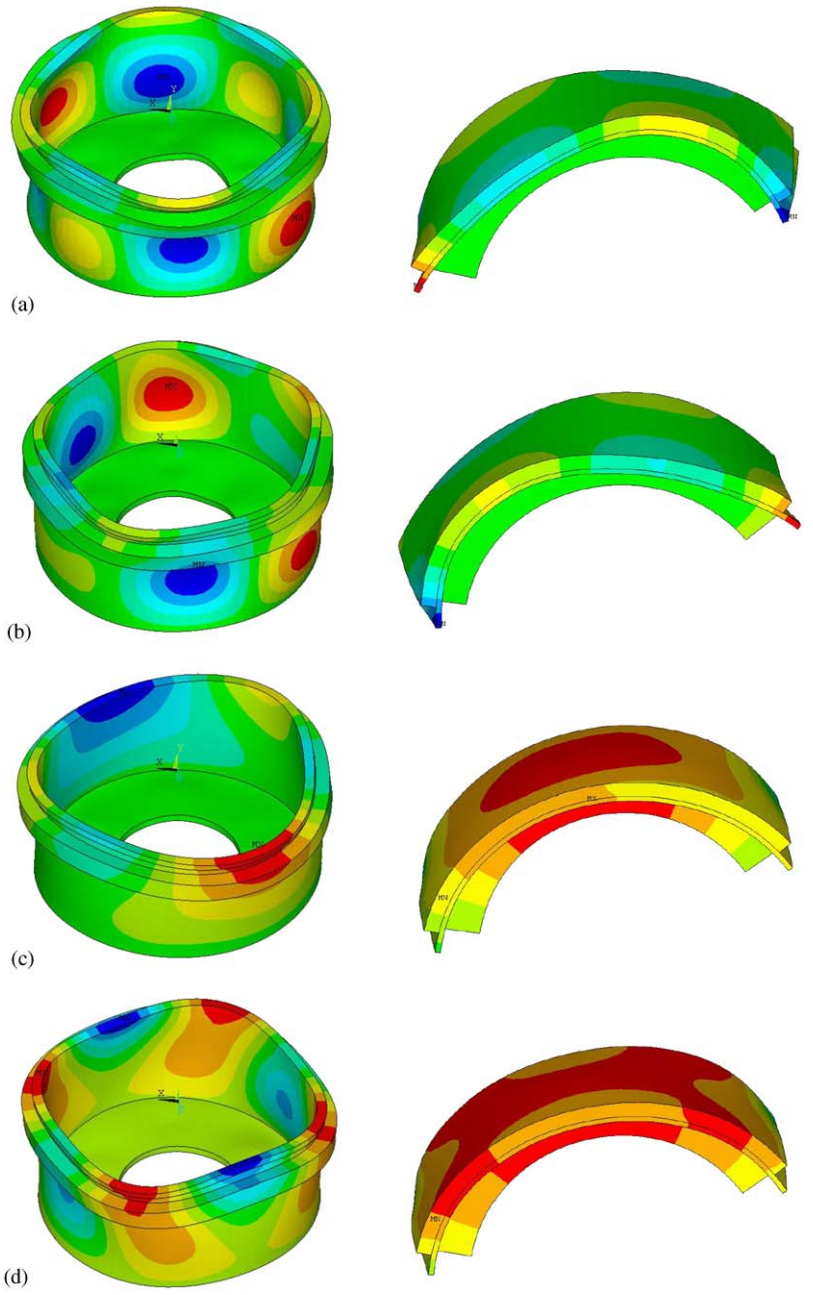

Fig. 8. Radial component of deformations for drum and shoe in mode shapes of the statically coupled brake system: (a) mode 29, (b) mode 30, (c) mode 31, (d) mode 32.

For each statically coupled mode for the system at $\mu = 0$, the mode shapes of the two shoes are either identical to each other or differ by a phase angle of 180°. The mode shapes of the shoes show a strong resemblance to those of the corresponding drum side wall where the two are in

contact through the lining. The statically coupled modes can be divided into two groups: in one group the two shoes (and also the parts of the drum side wall in contact with the shoes) move in the opposite radial direction (one moves outwards while the other moves inwards) as is the case with modes 30 and 31, while in the other group the two shoes move in the same radial direction as is the case with modes 29 and 32. All the modes in the same group will be termed "compatible", while the modes from different groups will be termed "incompatible". Compatible modes are more similar than incompatible modes at $\mu = 0$, and can quite possibly become identical when μ is increased. Incompatible modes such as modes 29 and 30, however, are never seen to combine to a merging state even though their frequency separation is quite small at $\mu = 0$.

It can be concluded that the modes should satisfy two conditions for them to merge: (1) the separation between the frequencies of two modes of a statically coupled system is sufficiently small, and (2) their component-wise mode shapes are compatible. When these two conditions are met, the two modes have a strong possibility to merge and cause squeal in the presence of friction coupling. Note that the friction coupling changes not only the natural frequencies of these modes but also their mode shapes so as to bring them closer and finally make them identical (both in frequency and in mode shape) at merging.

3.2. Influence of the lining stiffness

The effective stiffness of the lining material has a strong influence on the propensity to squeal in braking system for a number of reasons. Firstly, compression tests on friction lining material show that the Young's modulus of the lining material is dependent on the engagement pressure, with the material becoming stiffer at higher engagement pressures. Secondly, gradual wear of the lining material will reduce the lining thickness, and Eq. (2) shows that a decrease in lining thickness increases the effective lining stiffness. Thirdly, the lining stiffness is important in the stiffness and friction coupling of the drum and shoe modes. Brakes with different lining stiffness may have different squeal propensity. Hence, it is necessary and crucial to investigate the effect of the lining stiffness on the squeal propensity for the design of a quiet brake system.

Since the separation between the statically coupled frequencies is an important factor in determining the system stability characteristics, the influence of lining stiffness was first studied on the statically coupled frequencies. Then the friction was included in the system, and the changes in the value of $\mu_{\mathrm{cr,min}}$ with the changes in lining stiffness were studied. In order to explore the correlation between statically coupled frequencies and the stability boundaries defined by $\mu_{\mathrm{cr,min}}$, both results are plotted versus the normalized lining stiffness k in Fig. 9. Here k is a ratio of lining stiffness to nominal value of the lining stiffness per unit area and is defined by

$$k = \frac{E_{\mathrm{lin}}/h_{\mathrm{lin}}}{(E_{\mathrm{lin}}/h_{\mathrm{lin}})_{\mathrm{nominal}}}. \tag{12}$$

In the stiffness range from $k = 1.07$ to 1.11, the values of $\mu_{\mathrm{cr,min}}$ correspond to those due to the merging of modes 21 and 22. The separation between these two statically coupled frequencies reaches its smallest value at $k = 1.09$ and becomes larger away from this stiffness value. Correspondingly, the critical values of μ become minimum at $k = 1.09$ and increase on either side of this value. The modes 17 and 18 are found to merge and form the stability boundaries in the range from $k = 1.19$ to 1.26. They show the same behavior in that the minimal separation within

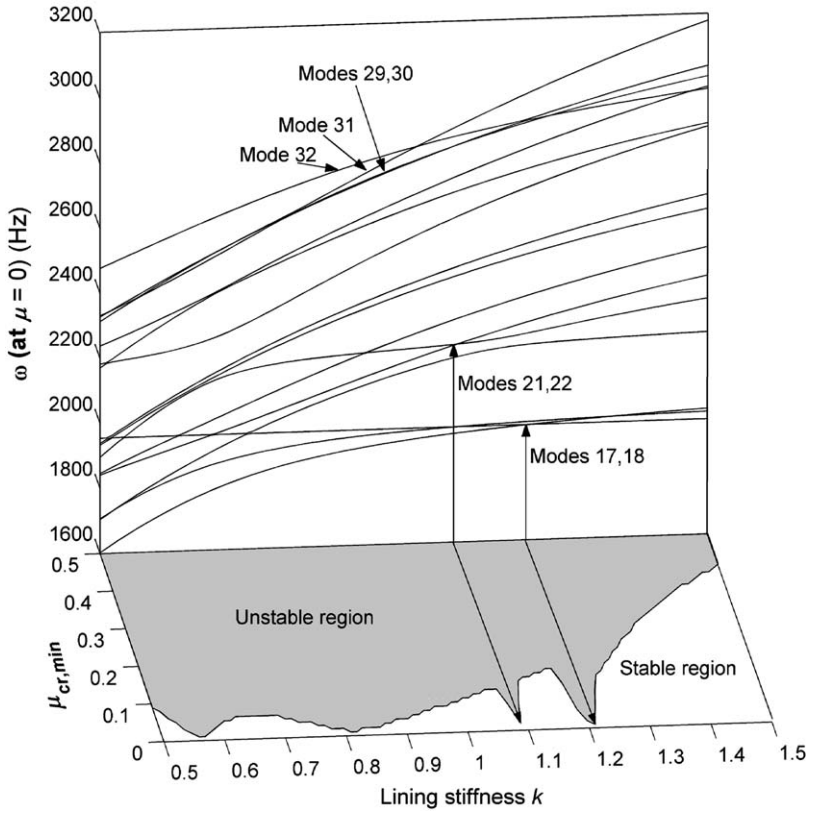

Fig. 9. Variation of the statically coupled natural frequencies and the critical friction coefficient $\mu_{cr,min}$ with the lining stiffness k.

the statically coupled frequencies corresponds to minimal critical value of μ. The mode pair 30 and 31 and the mode pair 29 and 32 with small frequency separations in the whole range are responsible for all the other values of $\mu_{cr,min}$ in Fig. 9. This clearly demonstrates that $\mu_{cr,min}$ and the corresponding pair of modes responsible for "coupled-mode" instability change with the variation of lining stiffness.

Though the separation within the statically coupled frequencies has a significant effect on the stability characteristics of the system, there are frequencies that intersect and have zero separation at some lining stiffness but do not lead to mode merging when friction is included in the coupled system. For example, the frequencies of modes 31 and 32 intersect at $k = 1.02$, but these two modes do not produce squeal. From the viewpoint of mode shapes, modes 31 and 32 are "incompatible". Now this phenomenon will be explained from the viewpoint of mode coupling.

Numerical results show that as a function of lining stiffness, the statically coupled modes of the brake assembly which tend to merge as the friction coefficient is increased are always associated with the phenomenon called "curve veering", while the modes which simply cross do not merge. In curve veering, two frequency loci (frequency curves as a function of some parameter) approach and then quickly diverge without intersection. An important feature of curve veering is that the

two eigenvalue curves do not actually intersect, and the two modes or eigenfunctions interact during veering in a rapid and continuous way. During curve crossing, however, the eigenfunctions interchange abruptly [20].

Traditionally the eigenvalue curve crossing and veering are illustrated by plotting eigenvalue loci versus a system parameter and checking whether the loci intersect or not. This method is not reliable since the observation is affected by the scale or resolution used to plot the figure. The "eigenfunction sensitivity" is presented here as a better way to distinguish between the "curve veering" and "curve crossing" behavior of modes. The sensitivity function for eigenvectors (or "eigenfunction sensitivity" in short) is defined as the inner product of ϕ_r and ϕ_s^0:

$$S_{rs} = \langle \phi_r, \phi_s^0 \rangle = (\phi_r)^{\mathrm{T}} \phi_s^0, \tag{13}$$

where ϕ_s^0 denotes the unperturbed sth eigenvector, and ϕ_r denotes the perturbed rth eigenvector at an adjacent lining stiffness when $\mu = 0$. The eigenvectors are normalized so that $(\phi_s^0)^{\mathrm{T}} \phi_s^0 = 1$ and $(\phi_r)^{\mathrm{T}} \phi_r = 1$. The values of S_{rs} are between 0 and 1, which represent the degree of resemblance between ϕ_r and ϕ_s^0.

The differences between curve veering and crossing are clearly illustrated in Figs. 10 and 11, in which the eigenfunction sensitivity is plotted with small variations of the lining stiffness k. In each figure, the values of inner products clearly show the changes of the eigenfunctions with the change in lining stiffness. In curve crossing there is no interaction between the two eigenfunctions and the two modes are totally independent of each other, while the two eigenvectors are almost interchanged during veering in a continuous way as the parameter k is varied.

When two statically coupled modes cross, their mode shapes are incompatible. Since there is no coupling between the modes showing curve crossing, no matter how small the separation is, they

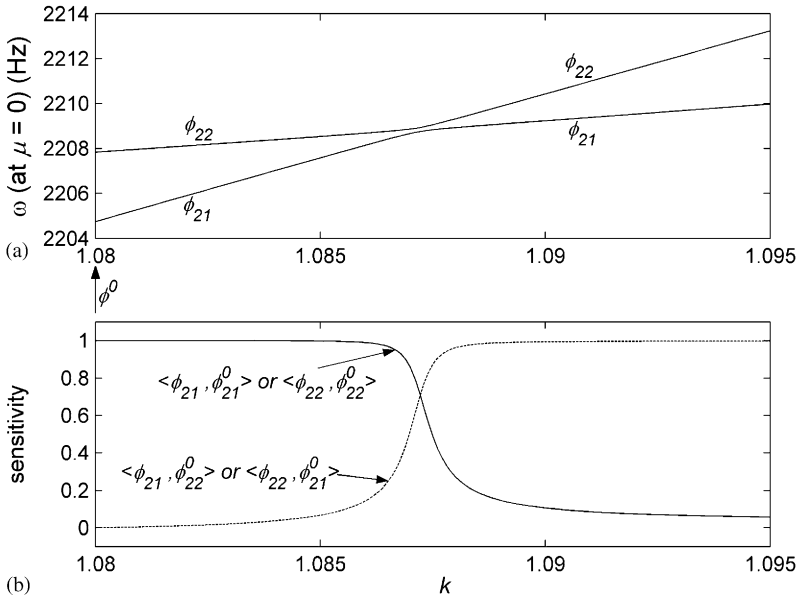

Fig. 10. (a) Frequency loci and (b) modal sensitivity functions for modes 21 and 22.

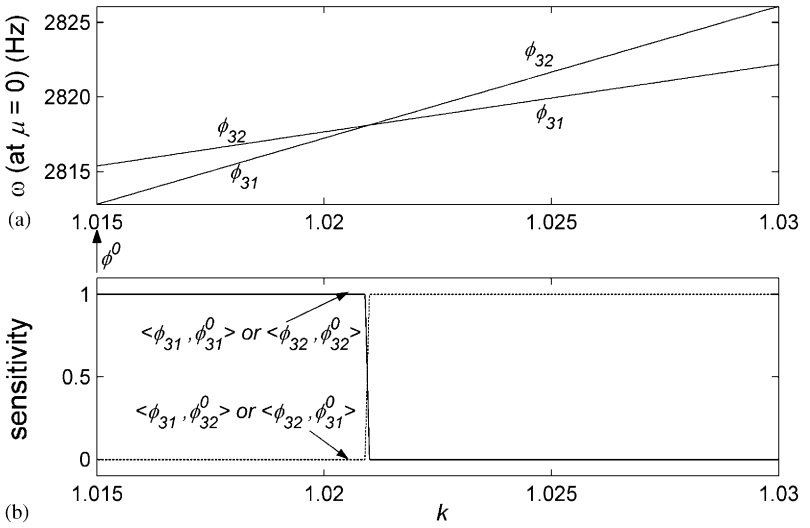

Fig. 11. (a) Frequency loci and (b) modal sensitivity functions for modes 31 and 32.

are not expected to merge or lead to instability when the friction is present in the system. When two statically coupled modes veer, their mode shapes are compatible. When coupling exists between two modes, the modes interact and they are likely to merge when friction exists and exceeds a critical value. This phenomenon of "eigenvalue veering" as an indicator of the possibility of merging of the corresponding eigenvalues to cause brake squeal was also seen for the case of disc brakes in Ref. [21].

It should be noted here that though the doublet modes due to symmetry of the drum may have small separation and come to merge, the drum modes with different orders are also possible to merge. Hence, dynamic instability is more general and more appropriate than binary flutter as the mechanism for brake squeal.

3.3. Effect of the hydraulic cylinder stiffness

To study the influence of the hydraulic cylinder stiffness k_h, four springs with constant stiffness are used to connect the ends of the shoes. The non-zero matrix $[C]$ is now included in the system model (10).

The calculations show that when k_h is less than 1×10^6 N/m, the stability characteristics of the coupled system are almost unaffected and the stability diagram is similar to Fig. 9. When k_h is increased beyond 1×10^6 N/m, the changes in the stability characteristics become significant. Fig. 12 shows the results for the case with $k_h = 6.5 \times 10^6$ N/m. Compared to Fig. 9, the statically coupled frequencies increase by different amounts so that the separation of the various frequencies change. The modes 21 and 22 still merge, but the corresponding instability region moves to left on the lining stiffness axis from its original location. The instability region resulting from the merging of modes 17 and 18 shifts left to a much larger extent.

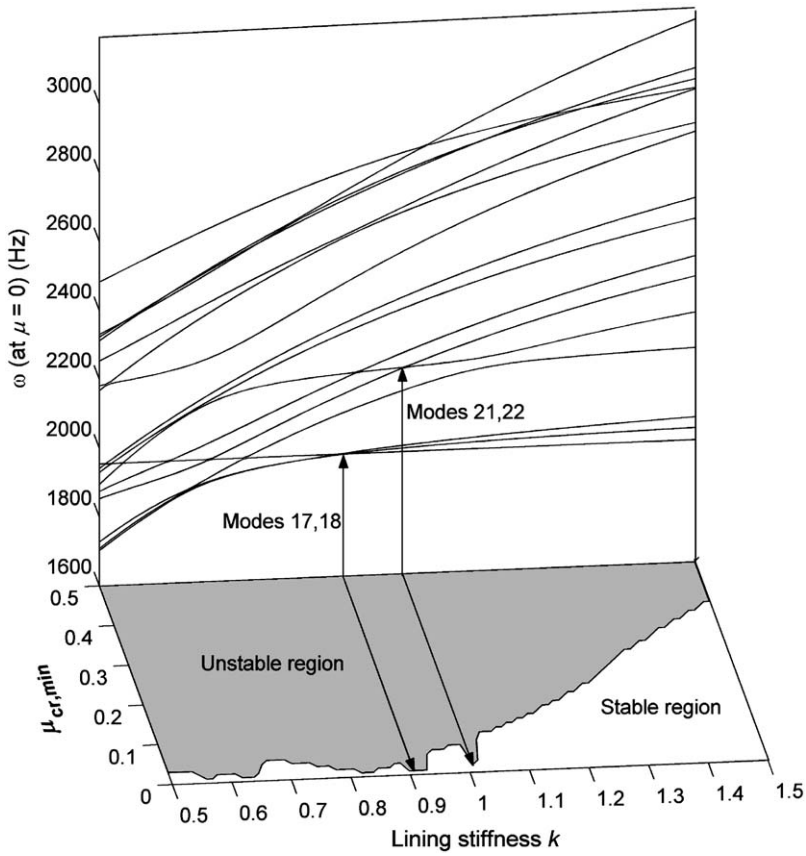

Fig. 12. Stability characteristics of a coupled drum brake system with hydraulic cylinder; $k_h = 6.5 \times 10^6$ N/m.

When the frequencies and modes ultimately responsible for squeal undergo small changes due to the variation of a parameter, the stability characteristics of the system may change dramatically. Some unstable regions may shift their locations or even disappear and some new unstable regions may be created because of the changes of the frequency separations. Hence, the instability regions are very sensitive to the changes in system parameters. This clearly points to the difficulties that arise in simulating practical brake systems because the system boundary conditions are not easily specified and therefore not easy to model accurately.

4. Conclusions and discussion

Brake squeal is a phenomenon of self-excited friction induced vibrations resulting from mode coupling. This paper presents an approach to develop a numerical drum brake model for squeal prediction, and analyzes the conditions that can lead to brake squeal. Based on the numerical model and results of complex eigenvalue analysis of the linear equations of motion, the following conclusions can be drawn:

(1) The component modal characteristics can be extracted from either analytical analysis or FE analysis. FE analysis makes it easy to capture geometry complexities of the components and incorporate the results of contact analysis in the system model. By creating virtual mesh of contact elements, the approach does not require the FE meshes of different components at the interfaces to match, thus greatly facilitating the FE modeling of the components.

(2) If the separation between the two modes due to static coupling is small enough and their mode shapes are compatible, the two modes have a good likelihood that they will merge when the friction is introduced and increased. Only compatible modes have the possibility to interact and become identical to result in instability. Though mode shapes of brake components are often measured with experimental methods, there are few investigations on the influence of mode shapes on mode merging. The understanding of the important role of mode shapes is expected to be of great help to prediction of the occurrence of squeal.

(3) The statically coupled modes which tend to merge in the presence of friction always exhibit curve veering phenomenon, while the modes which simply cross do not cause instability. There is no coupling between the statically coupled modes showing curve crossing. Curve veering reflects the coupling of compatible modes, and this coupling may cause the two modes to merge as the friction increases. Eigenvector sensitivity clearly allows for differentiation between modes that undergo curve crossing and those that undergo veering.

(4) The stability boundaries are sensitive to changes in parameters such as lining stiffness. Due to the correlation between the critical values of friction coefficient and the separations of the statically coupled frequencies, the changes in separations partially reveal the effects of the parameters on system stability and can provide an explanation to some squeal reduction techniques. These will be the subject of a work under preparation.

Acknowledgements

The first stage of the work was supported by Isuzu Motor Company, Ltd., and Dr. Hiroshi Takata was the project manager. The authors are also grateful for the support provided by Purdue Research Foundation.

References

[1] N.M. Kinkaid, O.M. O'Reilly, P. Papadopoulos, Automotive disc brake squeal: a review, *Journal of Sound and Vibration* 267 (1) (2003) 105–166.
[2] M. Nishiwaki, Generalized theory of brake noise, *Proceedings of the Institution of Mechanical Engineers* 207 (1993) 195–202.
[3] R.T. Spurr, A theory of brake squeal, *Proceedings of the Institution of Mechanical Engineers* 1 (1961–1962) 33–40.
[4] N. Millner, A theory of drum brake squeal, *Institute of Mechanical Engineering* C39/76 (1976) 177–185.
[5] M.R. North, A mechanism of disc brake squeal, *Proceedings of 14th International Automobile Technical Congress of FISTIA*, 1972, pp. 1/9–1/15.
[6] H. Okamura, M. Nishiwaki, A study on brake noise (drum brake squeal), *JSME International Journal, Series 3* 32 (2) (1989) 206–214.
[7] J. Hulten, Drum brake squeal—a self-exciting mechanism with constant friction, SAE Paper No. 932965, 1993.
[8] G.D. Liles, Analysis of disc brake squeal using finite element methods, SAE Paper No. 891150, 1989.

[9] D. Guan, D. Jiang, A study on disc brake squeal using finite element methods, SAE Paper No. 980597, 1998.
[10] H.V. Chowdhary, A.K. Bajaj, C.M. Krousgrill, An analytical approach to model disc brake system for squeal prediction, *Proceedings of DETC 2001/VIB-21560*, ASME, Pittsburgh, PA, 2001, pp. 1–10.
[11] H. Ouyang, Q. Cao, J.E. Mottershead, T. Treyde, Vibration and squeal of a disc brake: modelling and experimental results, *Proceedings of the Institution of Mechanical Engineers, Part D: Journal of Automobile Engineering* 217 (10) (2003) 867–875.
[12] T. Hamabe, I. Yamazaki, K. Yamada, H. Matsui, S. Nakagawa, M. Kawamura, Study of a method for reducing drum brake squeal, SAE Paper No. 1999-01-0144, 1999.
[13] W.V. Nack, Brake squeal analysis by finite element, *International Journal of Vehicle Design* 23 (3/4) (2000) 263–275.
[14] Y.S. Lee, P.C. Brooks, D.C. Barton, D.A. Crolla, A predictive tool to evaluate disc brake squeal propensity, Part 1: the model philosophy and the contact problem, *International Journal of Vehicle Design* 31 (3) (2003) 289–308.
[15] B.K. Servis, The Onset of Squeal Vibrations in Drum Brake Systems Resulting from a Coupled Mode Instability, Ph.D. Thesis, Purdue University, West Lafayette, IN, 2000.
[16] Y. Goto, T. Amago, K. Chiku, T. Matsushima, Y. Ishihara, Experimental identification method for contact stiffness between components of FE model for brake squeal, JSAE Paper No. 20045167, 2004.
[17] Z.B.M. Ripin, Analysis of Disc Brake Squeal using the Finite Element Method, Ph.D. Thesis, University of Leeds, Leeds, UK, 1995.
[18] P. Ioannidis, P.C. Brooks, D.C. Barton, Drum brake contact analysis and its influence on squeal noise prediction, SAE Paper No. 2003-01-3348, 2003.
[19] P. Dilisio, R. Parisi, J. Rieker, W. Stringham, Brake noise resolution on the 1998 Mercedes-Benz M-Class, SAE Paper No. 982245, 1998.
[20] N.C. Perkins, C.D. Mote Jr., Comments on curve veering in eigenvalue problems, *Journal of Sound and Vibration* 106 (1986) 451–463.
[21] H.V. Chowdhary, Modeling of Disc Brake Systems for Squeal Prediction, Master's Thesis, Purdue University, West Lafayette, IN, 2001.